Interaction between Cytochrome c_2 and the Photosynthetic Reaction Center from *Rhodobacter sphaeroides*: Role of Interprotein Hydrogen Bonds in Binding and Electron Transfer[†]

Edward C. Abresch, Mark L. Paddock, Miguel Villalobos, Charlene Chang, and Melvin Y. Okamura*

Department of Physics, University of California, San Diego, 9500 Gilman Drive, La Jolla, California 92093

Received September 3, 2008; Revised Manuscript Received October 27, 2008

ABSTRACT: The role of short-range hydrogen bond interactions at the interface between electron transfer proteins cytochrome c_2 (cyt) and the reaction center (RC) from *Rhodobacter sphaeroides* was studied by mutation (to Ala) of RC residues Asn M187, Asn M188, and Gln L258 which form interprotein hydrogen bonds to cyt in the cyt−RC complex. The largest decrease in binding constant K_A (8-fold) for a single mutation was observed for Asn M187, which forms an intraprotein hydrogen bond to the key residue Tyr L162 in the center of the contact region with a low solvent accessibility. Interaction between Asn M187 and Tyr L162 was also implicated in binding by double mutation of the two residues. The hydrogen bond mutations did not significantly change the second-order rate constant, k_2, indicating the mutations did not change the association rate for formation of the cyt−RC complex but increased the dissociation rate. The first-order electron transfer rate, k_e, for the cyt−RC complex was reduced by a factor of up to 4 (for Asn M187). The changes in k_e were correlated with the changes in binding affinity but were not accompanied by increases in activation energy. We conclude that short-range hydrogen bond interactions contribute to the close packing of residues in the central contact region between the cyt and RC near Asn M187 and Tyr L162. The close packing contributes to fast electron transfer by increasing the rate of electronic coupling and contributes to the binding energy holding the cyt in position for times sufficient for electron transfer to occur.

Interprotein electron transfer plays an important role in biological energy conversion in photosynthesis and respiration where mobile electron transfer proteins carry electrons between fixed membrane-bound protein complexes (*1*). The reaction between electron transfer partners requires binding followed by electron transfer processes that are governed by protein−protein interactions at the contact interface. These interactions can influence both the binding energy and pathway for electron transfer. The role of long-range electrostatic interactions has been extensively documented. However, short-range van der Waals and hydrogen bond interactions between proteins have not been as well studied. In this work, we examine the role of short-range interactions due to hydrogen bonds on the binding and electron transfer between cytochrome c_2 (cyt c_2)[1] and the reaction center (RC) from *Rhodobacter sphaeroides*.

The RC is a membrane-bound protein responsible for the initial light-induced electron transfer in photosynthesis (*2*). Light absorbed by the RC induces an electron transfer from a bacteriochlorphyll dimer, the primary electron donor D, through a series of intermediate acceptors to a quinone acceptor Q. Electrons from Q are passed through a cyclic electron transfer circuit involving cytochrome bc_1 and return to the RC carried by a water soluble electron carrier, cytochrome c_2 (*3*).

The reaction between cyt and RC has been extensively studied by pulsed laser kinetics experiments (*4*−*7*) which allow the determination of microscopic rate constants. The simplest scheme for the light-induced electron transfer reactions for RCs from *Rb. sphaeroides* is shown below.

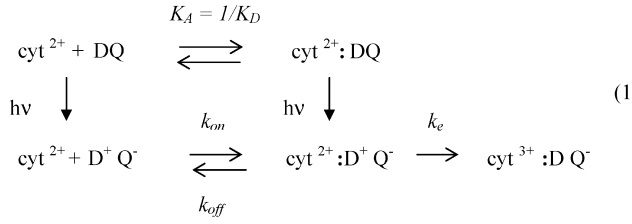

(1)

Prior to illumination, the reduced cyt and RC are in equilibrium between a bound and free state as shown in the top line (association constant $K_A = 1/K_D \sim 10^6$ M^{-1}). Light absorption leads to electron transfer forming the oxidized donor/reduced quinone acceptor D$^+$Q$^-$ pair (bottom line). In the fraction of RCs having a bound cyt, the first-order

[†] This work was supported by NIH Grant GM 41637. DNA sequencing was performed by the DNA Sequencing Shared Resource, UCSD Cancer Center, which is funded in part by NCI Cancer Center Support Grant 2 P30 CA23100-23.

* To whom correspondence should be addressed. Phone: (858) 534-2506. Fax: (858) 822-0007. E-mail: mokamura@ucsd.edu.

[1] Abbreviations: cyt c_2, cytochrome c_2; RC, reaction center; Q_0, 2,3-dimethoxy-5-methylbenzoquinone; D, primary electron donor (bacteriochlorophyll dimer); D$^+$, photo-oxidized primary electron donor; k_e, first-order electron transfer rate; k_2, second-order rate constant; k_{on}, association rate; k_{off}, dissociation rate; K_A, binding constant; K_D, dissociation constant; E_a, activation energy; $\Delta\Delta G$, change in binding free energy; SASA, solvent accessible surface area.

10.1021/bi801675a CCC: $40.75
Published on Web 11/20/2008

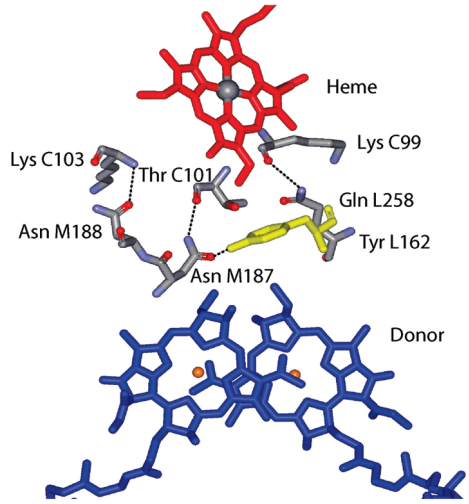

FIGURE 1: Structure of the cyt c_2−RC complex (PDB entry 1L9J) showing the interprotein hydrogen bonds (dotted lines) from three amide residues on the RC to backbone atoms on the bound cyt c_2. The redox active heme cofactor (red) on the cyt and the $BChl_2$ donor (blue) on the RC, buried in their respective proteins, are in close contact with the key RC residue, Tyr L162 (yellow), in the docked structure (*9*).

electron transfer reaction occurs on the time scale of microseconds ($k_e \sim 10^6\ s^{-1}$) (*4*). This reaction is rate-limited by electron tunneling as shown by its dependence on driving force (*8*). For the fraction of RCs lacking bound cyt, the reaction occurs via a second-order reaction k_2. For the reaction scheme shown in eq 1, the value of k_2 is governed by the equation

$$k_2 = \frac{k_e k_{on}}{k_{off} + k_e} \qquad (2)$$

where k_{on} and k_{off} are the association and dissociation rates, respectively (*1*). At low ionic strengths, $k_e \gg k_{off}$ and k_2 is in the diffusion limit $k_2 = k_{on} \sim 10^9\ s^{-1}\ M^{-1}$ (*4*). In this regime, electron transfer is limited by the rate of protein association and independent of electron transfer rate k_e, consistent with the finding that k_2 is independent of the driving force for electron transfer (*8*). The two key functional features of the reaction are that the diffusion-limited second-order rate constant is fast ($k_2 \sim 10^9\ s^{-1}\ M^{-1}$) and the dissociation rate of the cyt ($k_{off} \sim 10^3\ s^{-1}$) is fast enough not to be the rate-limiting step in turnover. These features are well optimized for cyclic electron transfer.

The molecular basis for these rates was revealed by the structure of the complex between cyt c_2 and RC from *Rb. sphaeroides* determined by X-ray crystallography (*9*). Measurement of the electron transfer rate in the cocrystal gave the same value as in solution ($k_e = 1.0 \times 10^6\ s^{-1}$), indicating that the cyt−RC complex in the crystal is in the active configuration. In the crystal structure, the cyt c_2 is bound on the surface of the RC with the redox active cofactors in the proximity of each other [heme edge close to $BChl_2$ (Figure 1)]. The interface region between the two proteins has a central short-range interaction domain with residues from the two proteins making van der Waals, cation−π, and hydrogen bond contacts. At the center of this domain is Tyr L162 on the RC which separates the two electron transfer cofactors (heme and $BChl_2$) and is a hot spot for binding and electron transfer in *Rb. sphaeroides* (*10, 11*). This region is surrounded by an electrostatic domain of solvent-separated charged residues which exhibit long-range electrostatic interactions.

The role of charged residues in the interface has been established by the dependence of electron transfer reaction rate k_2 on ionic strength (*12*), chemical modification of charged residues (*13*), cross-linking (*14, 15*), and site-directed mutagenesis of charged residues (*7, 16, 17*). Mutation of charged residues in the interface region changed K_A and k_2 but had little effect on k_e. The effects on K_A and k_2 were explained quantitatively by electrostatic interactions important for docking the positively charged heme-exposed surface of the cyt onto the negatively charged periplasmic side of the RC (*18, 19*). The lack of an effect on k_e shows that the electron tunneling interactions in the bound state were not changed via modification of charged residues in the peripheral electrostatic domain of the contact interface.

The role of short-range interactions was studied by mutation of hydrophobic residues (*10*) (*11*) and residues involved in the cation−π interaction (*20*). Mutation of hydrophobic residues changed both K_A and k_e. The changes in k_e show the importance of short-range tunneling contacts in the central region for electron transfer, particularly those involving Tyr L162 consistent with theoretical studies of electron transfer (*21*−*23*). The effect of hydrophobic mutations on k_2 was a function of the binding affinity of cyt c_2 for the mutant RC (*11*). For small changes in binding, k_2 was unchanged. However, if the binding affinity was reduced further, the value of k_2 decreased greatly. The pattern of changes to k_2 indicates that hydrophobic interactions do not alter k_{on} but have their major effect on k_{off}. The decrease in k_2 results when $k_{off} > k_e$ and dissociation occurs before electron transfer. The role of water molecules in the interface region in binding (*24, 25*) and electron transfer (*23*) has been studied.

What is the role of hydrogen bonding in interprotein electron transfer? An additional structural feature of the cyt−RC interface is the presence of interprotein hydrogen bonds between three amide residues (Asn M187, Asn M188, and Gln L258) on the RC and backbone atoms on cyt c_2 (Figure 1). In addition to interprotein hydrogen bonds, an intraprotein hydrogen bond is formed from Asn M187 to the critical Tyr L162 residue. To determine the role of these hydrogen bond interactions in the interprotein electron transfer process, we mutated the amide residues on the RC to Ala. To assess the role of the hydrogen bonding to Tyr L162, a double mutant having Tyr L162 → Phe and Asn M187 → Ala changes was constructed to compare with the single mutant RCs. The effect of these mutations on binding and electron transfer was studied using pulsed laser kinetics to study the role of hydrogen bonding in the dynamics and energy landscape for interprotein electron transfer. A preliminary report of this work has been presented (*26*).

MATERIALS AND METHODS

Site-Directed Mutagenesis. The site-directed mutations on the RC were constructed as previously described using the QuickChange mutagenesis kit (Stratagene) and a Perkin-Elmer PCR System (*27*). The mutation was confirmed by DNA sequencing.

Protein Isolation and Purification. The bacteria harboring the modified RC gene were grown in the dark as described previously (*27*). RCs from *Rb. sphaeroides* carotenoidless strain R26 (native) and mutant strains were isolated in 15 mM Tris-HCl (pH 8), 0.025% lauryl dimethylamine-*N*-oxide (LDAO), and 0.1 mM EDTA following published procedures (*27*). The final ratio of absorbance, A^{280}/A^{800}, was ≤1.5. The RC samples were then dialyzed for 2 days against HM [10 mM Hepes (pH 7.5) and 0.04% dodecyl β-D-maltoside (Anatrace)]. Native and mutant cyt c_2 proteins were isolated and purified as previously reported (*28*). Samples were purified to an absorbance ratio (A^{280}/A^{412}) of ≤0.3.

Quinone/Quinol Preparations. Quinone (Q_0) (2,3-dimethoxy-5-methylbenzoquinone) was obtained from Aldrich with a purity of ≥99%. Quinol (Q_0H_2) was synthesized by reducing quinone with hydrogen gas in the presence of platinum black, also obtained from Aldrich.

Electron Transfer Measurements. Electron transfer kinetics between the RC and cyt c_2 were measured by flash absorption spectroscopy by monitoring changes at 865 nm as described previously (*11*). For measurements of k_e in the microsecond range, absorbance changes were also monitored at 600 nm (to minimize the flash artifact) and a pulsed zenon flash was used as the source for the measuring beam to improve the signal-to-noise ratio. In the latter case, measurements were corrected for the small decay of the flash intensity during the measurement period. Most measurements were conducted at 23 °C in a buffer of 10 mM Hepes and 0.04% β-maltoside at pH 7.5. Samples included 50 μM Q_0 and Q_0H_2 as a redox buffer to ensure that the cyt c_2 was reduced prior to each laser flash. For measurements of the binding constant and second-order rate constant, a low RC concentration (<0.3 μM) was used to achieve a reasonably high fraction of unbound cyt and to prevent problems due to aggregation. For measurements of k_e, higher RC concentrations (~3 μM) were used to increase the signal-to-noise ratio necessary to measure the fast electron transfer rates.

The binding affinity and second-order rate constants were determined by monitoring the absorbance changes due to oxidation of D to D^+ at 865 nm. The association constant K_A was determined by monitoring the absorbance changes of the fast and slow phases (ΔA_f and ΔA_s, respectively) fit to the relation

$$\Delta A = \Delta A_f e^{-k_e t} + \Delta A_s e^{-k_s t} \quad (3)$$

where k_e is the fast rate constant associated with electron transfer from the bound cyt in the complex and k_s is the rate constant for the slow phase of electron transfer due to the association of the free cyt with the RC. The values of K_A were obtained from the fraction of bound cyt determined from the dependence of the amplitudes of the fast and slow phases on the concentration of free cyt.

$$\text{fraction bound} = \Delta A_f/(\Delta A_f + \Delta A_s) = 1/(1 + 1/K_A[\text{cyt}^{2+}]) \quad (4)$$

The change in free energy $\Delta\Delta G$ due to mutation of a residue is calculated by

$$\Delta\Delta G = k_B T \ln[K_A(\text{native})/K_A(\text{mutant})] \quad (5)$$

where k_B is Boltzmann's constant and T is the absolute temperature. The second-order rate constant, k_2, was determined from the observed rate of the slow phase of the electron transfer, k_s, under conditions where the concentration of free cyt c_2 was large compared to the unbound RC concentration, so that the reaction is pseudo-first-order. The rate constant k_s

$$k_s = k_2[\text{cyt}_{\text{reduced}}] \quad (6)$$

was plotted versus the free cyt c_2 concentration to yield the second-order rate constant, k_2.

Solvent Accessibility. The solvent accessible surface area (SASA) was determined for mutated residues in the structure of the cyt−RC complex using GETAREA version 1.1 (*29*) with a rolling ball with a radius of 1.4 Å.

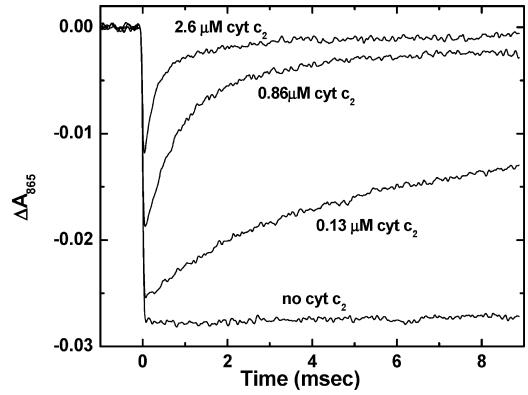

FIGURE 2: Absorbance changes due to electron transfer from cyt c_2 to the NA(M187) RC. In RC samples with no cyt c_2, oxidation of D (monitored at 865 nm) is observed after a laser flash at time zero with no recovery on this time scale. In the presence of cyt, two phases of recovery are observed: a fast phase near time zero, unresolved in these traces due to rapid electron transfer ($\tau \sim 4$ μs) from bound cyt (see Figure 4 for the resolution of this fast phase), and a slow phase due to second-order electron transfer from unbound cyt. The fraction of fast component and the rate of the slow phase increase with an increase in cyt concentration and were used to determine K_A and k_2. The RC concentration was 0.3 μM, and the values for the free cyt are as indicated. Conditions: 10 mM Hepes and 0.04% β-maltoside (pH 7.5) at 23 °C.

RESULTS

Flash Kinetics Experiment. The cytochrome binding and second-order rates of electron transfer were determined by laser kinetic experiments conducted at low RC concentrations (<0.3 μM) which weakened the effects of aggregation. A typical measurement is shown in Figure 2 for the NA(M187) [Asn M187 → Ala] mutant. The electron transfer from the RC to cyt was monitored by the recovery of the flash-induced absorbance at 865 nm. The reactions were biphasic. The fast phase is due to electron transfer from the fraction of RCs having a bound cyt (not resolved in Figure 2). The slow phase is due to the second-order reaction of the fraction of RCs lacking a bound cyt. The relative proportion of fast and slow phases was dependent on the cyt concentration and was used to determine the binding constant, K_A.

Effect of Mutations on the Binding Constant, K_A. The effects of mutating each of the hydrogen bonding residues (Asn M188, Gln L258, and Asn M187) on the RC surface to Ala resulted in different changes in binding constants (see Table 1). The largest change for single mutations was observed for mutation of Asn M187 (factor of 8) (Figure 3). The triple H-bond mutant [NA(M187)/NA(M188)/

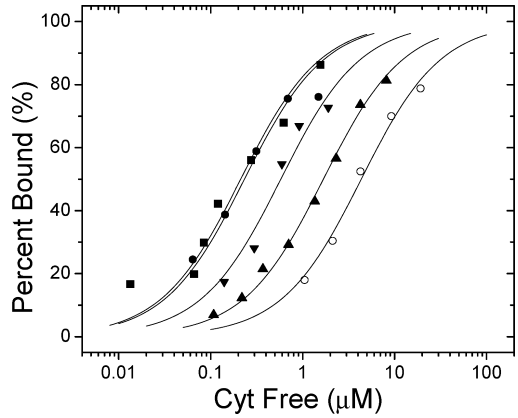

FIGURE 3: Plot of the fraction of RCs with bound cyt c_2 vs the free cyt c_2 concentration for native and mutant RCs: native (●), NA(M188) (■), QA(L258) (▼), NA(M187) (▲), and the triple mutant (○). The curves are the fits of eq 4 to the measured data for each RC. The values determined for K_A are listed in Table 1. The triple mutant has the largest decrease in binding affinity. Conditions: 0.2 μM RC in 10 mM Hepes and 0.04% β-maltoside (pH 7.5).

QA(L258)] having all three residues converted to Ala showed a larger decrease in K_A (factor of 18). The sum of the changes in free energies $\Delta\Delta G$ for the three single mutants (69 meV) is within uncertainty the same as the change in the free energy of the triple mutant (74 meV), indicating the additive effect of the individual mutations showing that these mutations act as independent contributions to the binding energy. The effects of the intraprotein hydrogen bond between Asn M187 and Tyr L162 was assessed by comparing the change in the binding energy of the double mutant YF(L162)/NA(M187) to that of the sum of the changes for single mutants. The double mutant had a change in free energy (64 meV) which was much smaller than the sum of the changes in free energy for the single mutants (126 meV). This indicates that the two residues do not affect binding independently to the cyt and suggest a role for an intraprotein hydrogen bond between Tyr L162 and Asn M187 in the binding process.

Effect of Mutations on the Second-Order Rate Constant, k_2. The rate of the slow phase of the electron transfer reaction shown in Figure 2 is proportional to the free cyt concentration and was used to determine the second-order rate constant. The second-order electron transfer rates were found to be relatively unchanged due to mutation of the hydrogen bonding residues (see Table 1). This is similar to the effect of mutating hydrophobic residues and can be explained if the short-range interactions are not yet formed in the transition state for rate-limiting protein association (*11*).

Effect of Hydrogen Bond Mutations on the Electron Transfer Rate in the Bound State, k_e. The fast kinetic data for the native RC and the NA M187 RC at a high cyt concentration (100 μM) monitored at 600 nm are shown in panels a and b of Figure 4. The NA(M187) RCs exhibited a significantly slower electron transfer rate than the native RC. The decays for both traces could be well fit by two exponential rate constants. For the NA(M187) RC, the fast-decaying major component (~80%) was assigned to the electron transfer rate in the bound state ($k_e = 2.5 \times 10^5$ s^{-1}), a reduction of 4-fold compared to

Table 1: Binding Constants, Free Energy Changes, Electron Transfer Rates, and Activation Energies for Native and Mutant RCs[a] and Solvent Accessible Surface Areas of the Mutated Residue[b]

RC strain	K_A (μM^{-1})	$\Delta\Delta G_B$ (meV)	k_e ($\times 10^6$ s^{-1})	E_a (meV)	k_2 ($\times 10^9$ s^{-1} M^{-1})	SASA (Å^2)
native	4.0	0	1.00	65	1.7	−
NA(M188)	5.0	−6	0.93	21	2.0	23
QA(L258)	1.7	22	0.82	5	1.4	14
NA(M187)	0.5	53	0.26	21	2.0	9
triple H-bond	0.22	74	0.10	35	1.5	−
YF(L162)	0.23	73	0.25	−	0.8	−
YF(L162)/NA(M187)	0.33	64	0.50	−	1.2	−

[a] K_A is the binding constant, k_e the first-order electron transfer rate constant, k_2 the second-order electron transfer rate constant, $\Delta\Delta G_B$ the change in the binding free energy with respect to the native RC, and E_a the activation energy for the first-order electron transfer rate. [b] SASA is the solvent accessible surface area of the mutated amino acid side chain in the native cyt−RC complex. Statistical uncertainties: measured rate constants are ±10%, K_A ± 10%, E_a ± 20 meV, $\Delta\Delta G_B$ ± 4 meV.

that of the native form. In addition, a small amount of slow component (~20%) was required to fit the data ($k_s = 5 \times 10^4$ s^{-1}). The fast rates were confirmed by taking data on multiple samples at both 600 and 865 nm. The triple H-bond mutant showed the greatest reduction in k_e (10-fold), and NA(M188) and QA(L258) exhibited a fast rate very similar to that of native RCs. The results are listed in Table 1.

The slow phase could be due to a small amount of a second-order phase or to heterogeneity. To test these ideas, the electron transfer rates were studied as a function of cyt concentration. The rate constant for the fast phase was independent of the cyt concentration, confirming the assignment to k_e (see Figure S1 of the Supporting Information). The rate constant for the slow phase was concentration-dependent and gave a k_{obs} of ~3×10^4 s^{-1} at a cyt concentration of 100 μM (see Figure S1 of the Supporting Information). This value is in the range of the observed values of k_s ($2-5 \times 10^4$ s^{-1}) seen in Figure 4. These results suggest that the slow phase at a high cyt concentration may be due to a small amount of second-order reaction.

The lack of saturation of the binding site even at a high cyt concentration may be due to aggregation of RC at the higher concentration of RCs necessary for fast electron transfer measurements. This aggregation may also account for the observation that full recovery of the signal to the baseline is not observed in some samples (e.g., Figure 4b). Evidence of aggregation comes from the finding that the amount of cyt needed to achieve half-saturation was greater at the high RC concentration needed to measure the fast kinetics than at the low concentrations used in the binding measurements (Figure S2 of the Supporting Information). This concentration dependence varied for different preparations of RC and is attributed to an aggregation of RCs that alters the cyt binding. Similar reports of aggregation of RCs have been described by Tiede (*30*).

Temperature Dependence of k_e. The activation energy, E_a, of k_e observed in native and hydrogen bond mutant RCs was determined by measuring the temperature dependence of the fast rate constant. As the temperature was lowered, the kinetic traces showed an increased amount of a slow phase (Figure 5). This result is due to a reduced level of binding of the cyt

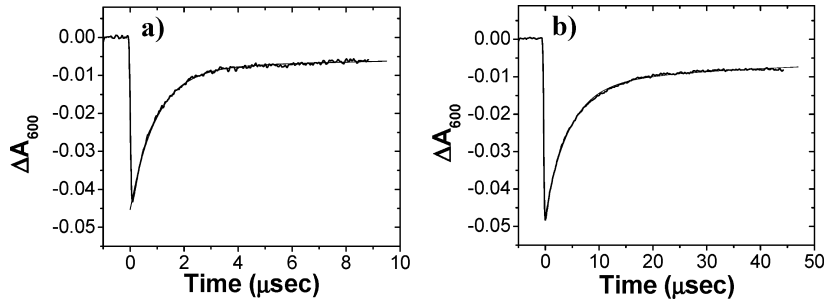

FIGURE 4: Absorbance changes due to electron transfer monitored at 600 nm for (a) native and (b) NA(M187) RCs in the presence of a high concentration of cyt c_2. The electron transfer rates in the mutant RCs were slower than in native RCs (note the difference in time scales). The concentration of the native RC was 3.5 μM and that of cyt 70 μM. The concentration of the NA(M187) RC was 4 μM and that of cyt 100 μM. The data were fit with eq 3. For native RCs, $k_e = 10^6$ s^{-1} (75%) and $k_s = 3 \times 10^4$ s^{-1} (25%), and for NA(M187) RCs, $k_e = 0.26 \times 10^6$ s^{-1} (80%) and $k_s = 5 \times 10^4$ s^{-1} (20%). Conditions: 10 mM Hepes and 0.04% β-maltoside (pH 7.5) at 26 °C).

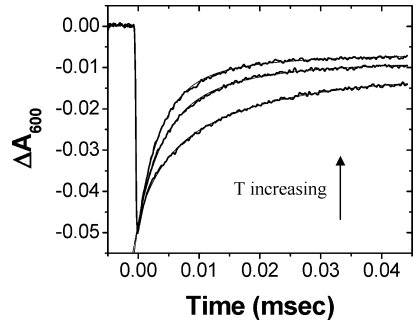

FIGURE 5: Temperature dependence of fast electron transfer between cyt and the NA(M187) RC. The data are shown for the electron transfer at 1, 18, and 36 °C (increasing from bottom to top). The decrease in rate at low temperatures is due mainly to a decrease in the fraction of RCs with bound cyt. The rate of the fast component was relatively temperature-independent (Figure 6). Other conditions were the same as those described in the legend of Figure 4.

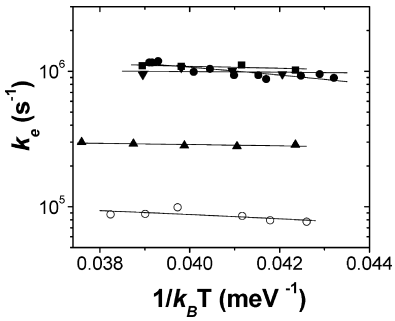

FIGURE 6: Plot of k_e vs $1/k_BT$ for native and mutant RCs: native (●), NA(M188) (■), QA(L258) (▼), NA(M187) (▲), and the triple mutant (○). The slope of the line fit to the data was used to obtain the activation energy E_a for electron transfer (Table 1). Conditions: 3 μM RC in 10 mM Hepes and 0.04% β-maltoside (pH 7.5).

at lower temperatures as shown by measurements made at lower RC and cyt concentrations (data not shown). The results indicate that the enthalpy for binding is positive ($\Delta H = +54 \pm 5$ meV for native RC, [RC] = 0.3 μM) and the binding is driven by entropy.

After correcting for the contribution due to the slow component, we found the values for k_e at different temperatures to be relatively temperature-independent. The activation energies, E_a, were calculated using the Arrhenius equation $k_e = k_o \exp(-E_a/k_BT)$ (see Figure 6). The values for the activation energies for k_e were all relatively low and were not increased by mutation of hydrogen bonds (Table 1). The activation energy for native RCs found in this study ($E_a = 65 \pm 12$ meV) is in good agreement with the activation energy ($E_a = 58$ meV) computed using the Marcus equation (*31*)

$$E_a = \frac{(\Delta G_e + \lambda)^2}{2k_BT} \quad (7)$$

using a λ value of 500 meV and a ΔG_e value of -160 meV (*8*). The activation energy measured here is lower than that obtained previously (*32*) under different conditions (60% glycerol), where a larger reorganization energy was measured ($\lambda = 1000$ meV) (*33*). A preliminary report (*34*) indicating larger activation energies for mutant RCs was in error, due to contributions from the second-order phase to the fast electron transfer reaction.

DISCUSSION

In this study, three residues on the RC surface that make interprotein H-bonds to cyt in the cyt−RC complex were mutated to Ala. The mutations were found to cause appreciable changes in binding affinity K_A, indicating a role of hydrogen bonds in binding. Although the mutations did not appreciably change the second-order rate constant, k_2, the rate of electron transfer between the two proteins in the bound state, k_e, decreased in parallel with decreasing binding affinity K_A. We argue below that the changes in electron transfer rate result from changes in the electronic coupling between cofactors, altered perhaps by changing the distances between contacts at the protein−protein interface. The altered distances appear to be correlated with the protein binding free energy.

Effects on Binding, K_A. The effects of mutating hydrogen-bonded residues resulted in a range of changes to the binding free energy (Table 1). The residue whose mutation produces the largest change in binding energy is Asn M187. This residue is unique is several respects. It is located near the center of the small cluster of residues that make hydrophobic contacts with the cyt (*9*). As a result, Asn M187 has a low solvent accessibility (SASA = 9 Å^2) in the cyt−RC complex (Table 1). In contrast, the other two residues are at the outer edge of the short-range contact domain and are much more solvent exposed (SASA = 14 and 23 Å^2). The changes in binding energy ($\Delta\Delta G$) are correlated with solvent accessibility (Table 1). This is consistent with the proposal that mutations of residues in solvent accessible regions may be compensated by interactions with solvent molecules with relatively little cost in energy, while mutation of deeply

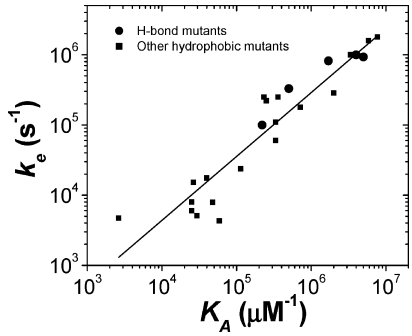

FIGURE 7: cyt c_2−RC first-order electron transfer rate constant k_e vs binding constant K_A for native and mutant RCs. The rates for H-bond mutants determined in this study (●) are plotted with rates previously determined (■) for hydrophobic mutant RCs (*11*). The H-bond mutants follow the same general trend in which changes in k_e are roughly proportional to changes in K_A.

buried residues necessarily entails a larger energy cost (*35, 36*). In addition, mutation of Asn M187 results in the loss of the intraprotein hydrogen bond to Tyr L162 (Figure 1) which may allow the phenolic ring to assume alternate configurations which could hinder cytochrome binding. The mobility of the aromatic residue may also account for the weakened binding of the YF(L162) mutant in which Phe replaces Tyr. The importance of the intraprotein hydrogen bond between Asn M187 and Tyr L162 is indicated by the finding that the change in binding energy for the double mutant YF(L162)/NA(M187) was smaller than the sum of energies for the single mutants (Table 1). This indicates that part of the effect of mutating Asn M187 is due to the steric interference with binding due to the increased mobility of the aromatic group.

In summary, the explanation for the large effect on binding due to mutation of Asn M187 is the energetic consequence of disruption of both intra- and interprotein closely packed contacts in the short-range interaction domain. The high specificity of the H-bond both in bond distance and in angle strongly restricts the structures capable of H-bond formation. The finding that H-bonds are involved in binding in the cyt−RC complex argues for the importance of a specific bound complex optimized for electron transfer.

Effects on the Second-Order Rate Constant, k_2. The second-order rate constant governs the maximum rate of turnover and can thus be viewed as controlling electron transfer in the biological system. The mutations of residues involved in H-bonding interactions do not appreciably change the second-order rate constant, k_2 (Table 1), indicating that these mutation have little effect on k_{on}. This is consistent with the model for the reaction in which the association rate k_{on} is the rate-limiting step and the transition state is one in which the cyt c_2 is located relatively far (∼10 Å) from the position in the bound state. Thus, in the transition state, the short-range interactions such as H-bonds have not yet been formed (*19*).

The main effect of short-range interactions such as hydrogen bonds is to decrease the dissociation rate, k_{off}. For small changes in k_{off}, the observed value of k_2 remains insensitive to changes in k_{off} as long as $k_{off} < k_e$. However, when $k_{off} > k_e$, as has been found for some of the more disruptive hydrophobic mutants (*11*), the second-order rate goes to a fast exchange regime in which dissociation occurs before electron transfer and the observed value of k_2 depends on the fraction of RC having a bound cyt in steady state equilibrium; i.e., $k_2 = k_e K_A$. Thus, short-range interactions such as H-bonds and hydrophobic interactions play an important role in electron transfer by retaining the cyt in the bound active configuration such that electron transfer occurs faster than dissociation. These features provide a measure of robustness to the interprotein electron transfer process.

Effects on the First-Order Electron Transfer Rate, k_e. The changes in k_e for different mutant RCs were roughly proportional to changes in K_A (see Table 1). These parallel changes in k_e and K_A due to mutation of hydrogen-bonding residues are similar to the changes previously observed due to mutation of hydrophobic residues involved in binding at the cyt−RC interface (*11*). The values of k_e and K_A resulting from mutation of hydrogen-bonding residues in this study are shown in Figure 7 together with the values resulting from mutation of hydrophobic residues.

The results indicate that the changes in k_e and K_A due to mutation of residues involved in short-range interactions are strongly correlated. How can this close correlation be explained? For conventional long distance electron tunneling, the rate is proportional to the electronic coupling (V) and the Franck−Condon factor (FC).

$$k_e = \frac{2\pi}{\hbar} V^2(\mathrm{FC}) \tag{8}$$

V decreases exponentially with distance (*37, 38*) while the main contribution to FC is $\exp(E_a/k_B T)$, where E_a varies with the free energy change upon electron transfer ΔG_e and reorganization energy λ as given in eq 7 (*31*). For changes to short-range interactions, i.e., hydrogen bonds and hydrophobic interactions, in the interface region of the cyt−RC complex, it is likely that the donor−acceptor distances would be altered. On the other hand, since the surface residues are relatively far from the cofactors and the mutations are rather conservative (i.e., they do not involve charged changes) and thus are expected to result in only small changes in the structure of the complex, the values of ΔG_e and λ (and thus FC) are not expected to change. A simple model for explaining the slower rates of electron transfer is one in which the donor−acceptor distance changes due to mutation. Such a change in distance would also affect the binding constant. However, there is no a priori reason to expect such a strong correlation between the electron transfer rate and binding constant over a wide range of mutations over an ∼20-fold change in the rate of electron transfer.

An alternative model to consider is a dynamic model in which the cyt binds in several conformations on the RC surface, each with different rates of electron transfer. Consequently, the rates and electron transfer parameters would depend on the dynamics and equilibria among the conformational states of the complex (*39*−*41*). One interesting possibility for explaining the lower rate of electron transfer is a dynamic docking model in which the conformation active in electron transfer has a higher energy than the conformation inactive in electron transfer. In this case, a lower rate of electron transfer would be associated with a larger activation energy. The results (Table 1) for the hydrogen bonding mutants indicate that this is not the case, and in fact for all mutant RCs, the activation energies are similar to and even slightly lower than that of the native RC. We thus conclude that the lower rate of electron transfer

in the hydrogen bond mutants occurs from the lowest-energy conformation of the cyt−RC complex. The low activation energies also rule out the possibility that the slower rates are due to changes in driving force or reorganization energy. Thus, the slower rates in the mutant RCs are due to weaker electronic coupling interaction V between heme and $BChl_2$ in the cyt−RC complex.

The correlation between the electron transfer rate and binding changes remains to be explained quantitatively at the molecular level. Possible approaches to gain insight include detailed electron tunneling pathway calculations (*38*) using static or dynamic models. The binding energy should include contributions from short-range interaction, electrostatic interactions, and desolvation (*18*). The rate may be influenced by electron transfer through solvent water at the interface (*23, 42*) or the dynamics of conformational interconversion in a reaction−diffusion model (*43*). Further studies of this problem may provide insights into the structure and dynamics of short-range protein−protein interactions.

CONCLUSIONS

Mutation of hydrogen-bonded residues, particularly Asn M187 which is closely associated with Tyr L162, in the interface region in the cyt−RC complex shows that these residues play a role in binding of the cyt to the RC in a position for fast electron transfer. Hydrogen bonding facilitates the close contact and tight packing at the interface leading to strong electronic coupling resulting in fast electron transfer. The hydrogen bonds do not greatly affect the rate of association of the cyt with the RC but play a significant role in decreasing the dissociation rate and thus allow the cyt to be bound long enough for electron transfer in the complex to occur. These results show the importance of short-range interactions in the interprotein electron transfer process.

ACKNOWLEDGMENT

We thank Osamu Miyashita and Jose Onuchic for helpful discussions of electron transfer theory.

SUPPORTING INFORMATION AVAILABLE

Biphasic electron transfer rates versus cyt c_2 concentration for NA(M187) and triple mutant RCs (Figure S1) and K_D as a function of RC concentration (Figure S2). This material is available free of charge via the Internet at http://pubs.acs.org.

REFERENCES

1. Bendall, D. (1996) in *Protein electron transfer* (Bendall, D., Ed.) pp 43−68, Bios Scientific Publishers Ltd., Oxford, U.K.
2. Blankenship, R. E. (2002) *Molecular mechanisms of photosynthesis*, Blackwell Science Inc., London.
3. Dutton, P. L., and Prince, R. C. (1978) in *The photosynthetic bacteria* (Clayton, R. K., and Sistrom, W. R., Eds.) pp 525−570, Plenum Press, New York.
4. Tiede, D., and Dutton, P. (1993) in *The photosynthetic reaction center* (Deisenhofer, J., and Norris, J., Eds.) pp 258−288, Academic Press, San Diego.
5. Overfield, R. E., Wraight, C. A., and Devault, D. C. (1979) Microsecond photooxidation kinetics of cytochrome c2 from *Rhodopseudomonas sphaeroides*: In vivo and solution studies. *FEBS Lett. 105*, 137–142.
6. Moser, C., and Dutton, P. L. (1988) Cytochrome c and c2 binding dynamics and electron transfer with photosynthetic reaction center protein and other integral membrane redox proteins. *Biochemistry 27*, 2450–2461.
7. Tetreault, M., Rongey, S. H., Feher, G., and Okamura, M. (2001) Interaction between cytochrome c2 and the photosynthetic reaction center from *Rhodobacter sphaeroides*: Effects of charge-modifying mutations on binding and electron transfer. *Biochemistry 40*, 8452–8462.
8. Lin, X., Williams, J. C., Allen, J., and Mathis, P. (1994) Relationship between rate and free energy difference for electron transfer from cytochrome c2 to the reaction center in *Rhodobacter sphaeroides*. *Biochemistry 33*, 13517–13523.
9. Axelrod, H. L., Abresch, E. C., Okamura, M. Y., Yeh, A. P., Rees, D. C., and Feher, G. (2002) X-ray structure determination of the cytochrome c2: Reaction center electron transfer complex from *Rhodobacter sphaeroides*. *J. Mol. Biol. 319*, 501–515.
10. Farchaus, J., Wachtveitl, J., Mathis, P., and Oesterhelt, D. (1993) Tyrosine 162 of the photosynthetic reaction center l-subunit plays a critical role in the cytochrome c2 mediated rereduction of the photooxidized bacteriochlorophyll dimer in *Rhodobacter sphaeroides*. 1. Site-directed mutagenesis and initial characterization. *Biochemistry 32*, 10885–10893.
11. Gong, X., Paddock, M., and Okamura, M. (2003) Interactions between cytochrome c2 and photosynthetic reaction center from *Rhodobacter sphaeroides*: Changes in binding affinity and electron transfer rate due to mutation of interfacial hydrophobic residues are strongly correlated. *Biochemistry 42*, 14492–14500.
12. Prince, R. C., Cogdell, R. J., and Crofts, A. R. (1974) The photo-oxidation of horse heart cytochrome c and native cytochrome c2 by reaction centres from *Rhodopseudomonas spheroides* r-26. *Biochim. Biophys. Acta 347*, 1–13.
13. Long, J., Durham, B., Okamura, M., and Millett, F. (1989) Role of specific lysine residues in binding cytochrome c2 to the *Rhodobacter sphaeroides* reaction center in optimal orientation for rapid electron transfer. *Biochemistry 28*, 6970–6974.
14. Drepper, F., Dorlet, P., and Mathis, P. (1997) Cross-linked electron transfer complex between cytochrome c2 and the photosynthetic reaction center of *Rhodobacter sphaeroides*. *Biochemistry 36*, 1418–1427.
15. Rosen, D., Okamura, M. Y., Abresch, E. C., Valkirs, G. E., and Feher, G. (1983) Interaction of cytochrome c with reaction centers of rhodopseudomonas sphaeroides r-26: Localization of the binding site by chemical cross-linking and immunochemical studies. *Biochemistry 22*, 335–341.
16. Caffrey, M. S., Bartsch, R. G., and Cusanovich, M. A. (1992) Study of the cytochrome c2-reaction center interaction by site-directed mutagenesis. *J. Biol. Chem. 267*, 6317–6321.
17. Tetreault, M., Cusanovich, M., Meyer, T., Axelrod, H., and Okamura, M. (2002) Double mutant studies identify electrostatic interactions that are important for docking cytochrome c2 onto the bacterial reaction center. *Biochemistry 41*, 5807–5815.
18. Miyashita, O., Onuchic, J. N., and Okamura, M. Y. (2003) Continuum electrostatic model for the binding of cytochrome c2 to the photosynthetic reaction center from *Rhodobacter sphaeroides*. *Biochemistry 42*, 11651–11660.
19. Miyashita, O., Onuchic, J., and Okamura, M. (2004) Transition state and encounter complex for fast association of cytochrome c2 with bacterial reaction center. *Proc. Natl. Acad. Sci. U.S.A. 101*, 16174–16179.
20. Paddock, M., Weber, K., Chang, C., and Okamura, M. (2005) Interactions between cytochrome c2 and the photosynthetic reaction center from *Rhodobacter sphaeroides*: The cation-π interaction. *Biochemistry 44*, 9619–9625.
21. Aquino, A., Beroza, P., Beretan, D., and Onuchic, J. (1995) Docking and electron transfer between cytochrome c2 and the photosynthetic reaction center. *Chem. Phys. 197*, 277–288.
22. Miyashita, O., Okamura, M. Y., and Onuchic, J. N. (2003) Theoretical understanding of the interprotein electron transfer between cytochrome c_2 and the photosynthetic reaction center. *J. Phys. Chem. B 107*, 1230–1241.
23. Miyashita, O., Okamura, M., and Onuchic, J. (2005) Interprotein electron transfer from cytochrome c_2 to photosynthetic reaction center: Tunneling across an aqueous interface. *Proc. Natl. Acad. Sci. U.S.A. 102*, 3558–3563.
24. Pogorelov, T., Autenrieth, F., Roberts, E., and Luthey-Schulten, Z. (2007) Cytochrome c_2 exit strategy: Dissociation studies and evolutionary implications. *J. Phys. Chem. B 111*, 618–634.

25. Autenrieth, F., Tajkhorshid, E., Schulten, K., and Luthey-Schulten, Z. (2004) Role of water in transient cytochrome c2 docking. *J. Phys. Chem. B 108*, 20376–20387.
26. Abresch, E., Villalobos, M., Paddock, M., Chang, C., and Okamura, M. (2006) The importance of buried H-bonds on binding and electron transfer in the cytochrome c2:reaction center complex, 2006 Biophysical Society Annual Meeting Abstract. *Biophys. J. 90*, 770-Plat.
27. Paddock, M. L., Adelroth, P., Chang, C., Abresch, E. C., Feher, G., and Okamura, M. Y. (2001) Identification of the proton pathway in bacterial reaction centers: Cooperation between Asp-m17 and Asp-l210 facilitates proton transfer to the secondary quinone (q(b)). *Biochemistry 40*, 6893–6902.
28. Bartsch, R. (1978) in *The photosynthetic bacteria* (Clayton, R., and Sistrom, W., Eds.) pp 249−279, Plenum Press, New York.
29. Fraczkiewicz, R., and Braun, W. (1998) Exact and efficient analytical calculation of the accessible surface areas and their gradients for macromolecules. *J. Comput. Chem. 19*, 319–333.
30. Tiede, D. M., Littrell, K., Marone, P. A., Zhang, R., and Thiyagarajan, P. (2000) Solution structure of a biological bimolecular electron transfer complex: Characterization of the photosynthetic reaction center-cytochrome c2 protein complex by small angle neutron scattering. *J. Appl. Crystallogr. 33*, 560–564.
31. Marcus, R. A., and Sutin, N. (1985) Electron transfer in chemistry and biology. *Biochim. Biophys. Acta 811*, 265–322.
32. Venturoli, G., Mallardi, A., and Mathis, P. (1993) Electron transfer from cytochrome c2 to the primary donor of *Rhodobacter sphaeroides* reaction centers. A temperature dependence study. *Biochemistry 32*, 13245–13253.
33. Venturoli, G., Drepper, F., Williams, J., Allen, J., Lin, X., and Mathis, P. (1998) Effects of temperature and ΔG^0 on electron transfer from cytochrome c2 to the photosynthetic reaction center of the purple bacterium *Rhodobacter sphaeroides*. *Biophys. J. 74*, 3226–3240.
34. Abresch, E., Paddock, M., and Okamura, M. Y. (2007) Inter-protein electron transfer from cytochrome c2 to reaction center: Electron transfer in the bound complex reflects dynamic conformational fluctuations, 2007 Biophysical Society Meeting Abstracts. *Biophys. J.,* 503a.
35. Bogan, A., and Thorn, K. (1998) Anatomy of hot spots in protein interfaces. *J. Mol. Biol. 280*, 1–9.
36. Lo Conte, L., Chothia, C., and Janin, J. (1999) The atomic structures of protein-protein recognition sites. *J. Mol. Biol. 285*, 2177–2198.
37. Moser, C. C., Keske, J. M., Warnke, K., Farid, R. S., and Dutton, P. L. (1992) The nature of biological electron transfer. *Nature 355*, 796–802.
38. Beratan, D., Betts, J., and Onuchic, J. (1991) Protein electron transfer rates set by the bridging secondary and tertiary structure. *Science 252*, 1285–1288.
39. Zhou, J. S., and Kostic, N. M. (1992) Photoinduced electron transfer from zinc cytochrome c to plastocyanin is gated by surface diffusion within the metalloprotein complex. *J. Am. Chem. Soc. 114*, 3562–3563.
40. Davidson, V. L. (2000) Effects of kinetic coupling on experimentally determined electron transfer parameters. *Biochemistry 39*, 4924–4928.
41. Liang, Z. X., Kurnikov, I. V., Nocek, J. M., Mauk, A. G., Beratan, D. N., and Hoffman, B. M. (2004) Dynamic docking and electron-transfer between cytochrome b5 and a suite of myoglobin surface-charge mutants. Introduction of a functional-docking algorithm for protein-protein complexes. *J. Am. Chem. Soc. 126*, 2785–2798.
42. Lin, J., Balabin, I., and Beratan, D. (2005) The nature of aqueous tunneling pathways between electron-transfer proteins. *Science 310*, 1311–1313.
43. Wang, H., Lin, S., Allen, J., Williams, J., Blankert, S., Laser, C., and Woodbury, N. (2007) Protein dynamics control the kinetics of initial electron transfer in photosynthesis. *Science 316*, 747–750.

BI801675A